Received: 8 December 2023 | Revised: 1 March 2024 | Accepted: 4 March 2024 | Published online: 18 March 2024

RESEARCH ARTICLE

Journal of Optics and Photonics Research
2025, Vol. 00(00) 1–11
DOI: 10.47852/bonviewJOPR42022256

BON VIEW PUBLISHING

Instigating the Asymmetry of Dy^{3+} Ions Doped in Borate Glasses for Photonic Device *w*-LED Applications

Basavaraj Gurav[1], G. B. Devidas[1], Ashok Dinkar[1], Darya Pavlovna Surzhikova[2] and R. Rajaramakrishna[2,*]

[1]*Department of Physics, Kuvempu University, India*

[2]*Siberian Federal University, Russia*

Abstract: For usage in solid-state white light-emitting device applications, dysprosium-activated calcium aluminum barium sodium borate glass was synthesized. The detailed understanding of physical, optical, structural, and photoluminescence characteristics was examined and compared. To comprehend the oscillator strength of the ligands in the prepared glasses, the Judd–Ofelt intensity characteristics were assessed. The Ω_2 greater relative oscillator strength value shows highest for the prepared glasses suggesting their cause due to hypersensitive transitions. In comparison to other glasses in the research, the potential radiative transition probabilities, branching ratios, and stimulated emission cross-section for 575 nm emission all exhibited higher values. The stimulated emission cross-section shows highest for 0.3 mol% Dy_2O_3 content in the present glasses. The asymmetry of synthesized glass sample ratio has been evaluated and compared using yellow to blue (Y/B) emission ratio. Study of the emission spectra and assessment of co-related color temperature and D_{uv} values for the glasses reveal emission in the CIE diagram's white light zone.

Keywords: Dy^{3+} ions, JO-theory, radiative properties, borate glass, CIE diagram

1. Introduction

The Dy^{3+} ion has a remarkable fluorescence performance in the region of white light emission, making it one of the most fascinating rare-earth ions (REIs) for doping in glasses [1]. One of the REIs, trivalent dysprosium Dy^{3+}, has the potential to be used in white light applications [2]. A fascinating oxide that has been discovered to be more efficient in optical applications owing to an increase in fluorescence when doped in host materials is the different glass intermediates, such as Al_2O_3 [3]. To increase the stability of the glass network, borate as a glass forming still has to be mixed with other oxide modifiers, such as alkaline oxides. Dy^{3+} doped glass is more intriguing to research due to its high emission in the visible range of 400–800 nm, and the impact of the CaO component on luminescence qualities was also studied [4, 5]. The line linking the blue and yellow sections in the CIE 1931 chromatic diagram often passes through the zone of white light. White light quality may be predicted from the material by adjusting the intensity of yellow to blue (Y/B) emission [6]. Glasses made of $23CaO + 10Al_2O_3 + (51–x)B_2O_3 + 6BaO + 10Na_2O + xDy_2O_3$ (where $x = 0.1$, 0.3, 0.5, and 1.0 mol%) were described in the paper, and their optical characteristics were assessed using Judd–Ofelt analysis. The present stoichiometry was chosen because the addition of BaO and Al_2O_3 content to the glass would increase the stability and also influence the structure's compactness. The emission of yellow and blue light obtained by the Dy_2O_3 content which can be tailored to produce superior white light by analyzing their asymmetry ratio in the host matrix. In the present work, the key impact of the novel glass which has studied shows superior photonic white emission compared with other reported literatures.

2. Experimental Methods

2.1. Glass preparation

Glass samples were synthesized by melt quenching method, with a composition of $23CaO + 10Al_2O_3 + (51–x)B_2O_3 + 6BaO + 10Na_2O + xDy_2O_3$. The high-quality oxide chemicals $CaCO_3$, Al_2O_3, H_3BO_3, $BaCO_3$, Na_2CO_3, and Dy_2O_3 were thoroughly combined in a pestle and mortar before being crushed to a fine powder and weighed at 15 g. The resultant mixture was then cooked for 3 hours at 1150 °C in an electrical furnace. The glass was then annealed for the full day at 550 °C before being allowed to cool gradually to ambient temperature. The refractive index was measured using digital Abbe refractometer at sodium wavelength (589.3 nm) with 1-bromonaphthalin ($C_{10}H_7Br$) as contact liquid. The density of the glass was determined by Archimedes' method, using distilled water as an immersion liquid. Furthermore, the molar volume is calculated based on the density data. The absorption spectrum characterization was conducted using the Shimadzu 3600 UV-VIS-NIR spectrophotometer. Meanwhile, excitation and emission spectra were observed using the Agilent Cary Eclipse spectrofluorometer. The prepared glasses are shown in Figure 1, and their glass stoichiometry ratio with glass code is presented in Table 1.

*Corresponding author: R. Rajaramakrishna, Siberian Federal University, Russia. Email: rrajanavaneethakrishna@sfu-kras.ru

Figure 1
Prepared glass samples

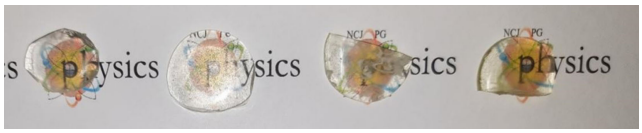

Table 1
Glass samples with different compositions

Samples	Glass composition (mol%)
(D1) CaAlBBaNaDy (0.1)	23CaO-10Al_2O_3-50.9B_2O_3-6BaO-10Na_2O-0.1Dy_2O_3
(D2) CaAlBBaNaDy (0.3)	23CaO-10Al_2O_3-50.7B_2O_3-6BaO-10Na_2O-0.3Dy_2O_3
(D3) CaAlBBaNaDy (0.5)	23CaO-10Al_2O_3-50.5B_2O_3-6BaO-10Na_2O-0.5Dy_2O_3
(D4) CaAlBBaNaDy (1.0)	23CaO-10Al_2O_3-50.0B_2O_3-6BaO-10Na_2O-1.0Dy_2O_3

3. Result and Discussion

3.1. Physical properties

3.1.1. Analysis of density, molar volume, and dielectric constant

The density (ρ) and molar volume of produced glass were calculated [6]. Table 2 lists the physical properties of the prepared glass sample and the refractive index of the glass with variation of Dy content are shown in Figure 2. When the mol% concentration of Dy_2O_3 in the glass increases, the molar volume rises from 2.4738 (gm/kg^3) to 2.8424 (gm/kg^3) and from 25.5086 (cm^3/mol) to 34.442 (gm/kg^3), which is shown in Figure 3. The increase in glass density may be attributed to Dy_2O_3 increased molecular weight (372.998 g/mol), which is higher than the molecular weights of the other components in the glass samples. (CaO, Al_2O_3, B_2O_3, BaO, and Na_2O have respective molecular weights of 56.08, 101.96, 69.6203, 153.33, and 61.9789 g/mol) which is less than the rare-earth molecular weight. As a result, when Dy^{3+} ions are alternately exchanged with B_2O_3, the glass matrix becomes denser. In contrast, D2 glass exhibits lower density and larger volume when compared to other glasses, indicating that the glass contains more nonbridging oxygen. The increase in molar volume in the glass samples might be attributed to the formation of non-bonding oxygen (NBO) and the growth of the calcium aluminum barium sodium borate glass network. By increasing the Dy_2O_3 concentration in the glass samples, the dielectric constant is substantially raised [7].

Table 2
Physical properties of D series with different Dy_2O_3 concentration

Physical properties	D1	D2	D3	D4
Density (g/cm^3)	2.4738	2.1746	2.9603	2.8424
Molar volume (cm^3/mol)	29.783	34.442	25.5086	27.219
Refractive index (n)	1.58	1.58	1.57	1.58
Dielectric constant (ε)	2.496	2.496	2.496	2.496
Dy^{3+}ion concentration ($\times10^{21}$ ions/cm^3)	0.551	1.429	3.217	6.031
Polaon radius r_p (A°)	5.018	3.653	2.789	2.262
Interionic distance r_i (A°)	1.222	0.889	0.678	0.550
Field strength ($F \times 10^{20}$) cm^{-2}	0.148	0.279	0.479	0.728
Average boron–boron separation (d_{B-B}) (A°)	3.931	3.957	3.992	4.031
Molar refraction (R) (cm^3/mol)	9.9120	11.4624	8.3691	9.0586
Molar cation polarizability (α_{cat})	0.253	0.253	0.253	0.253
No. of oxides in chemical formula ($N_O{}^{2-}$)	2.22	2.22	2.22	2.22
Electronic oxide polarizability ($\alpha_o{}^{2-}$)	1.657	1.934	1.381	1.504
Optical basicity (Λ)	0.6035	0.5170	0.7241	0.6648
Metallization criteria (M)	0.667	0.667	0.671	0.667
Theoretical basicity (Λ_{theo})	0.691	0.690	0.689	0.687

Figure 2
Refractive index vs concentration of Dy_2O_3 content

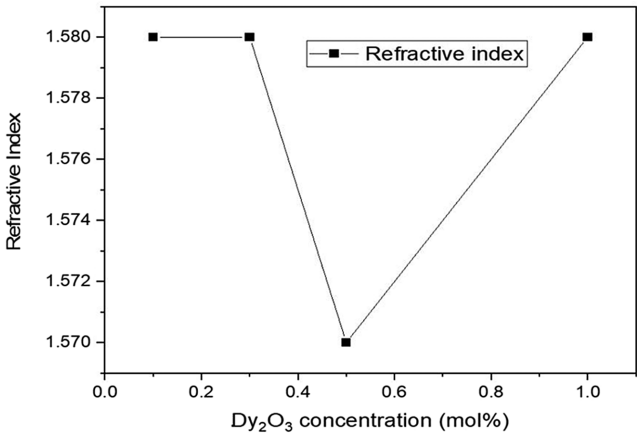

Figure 3
Density, molar volume vs concentration of Dy_2O_3 content

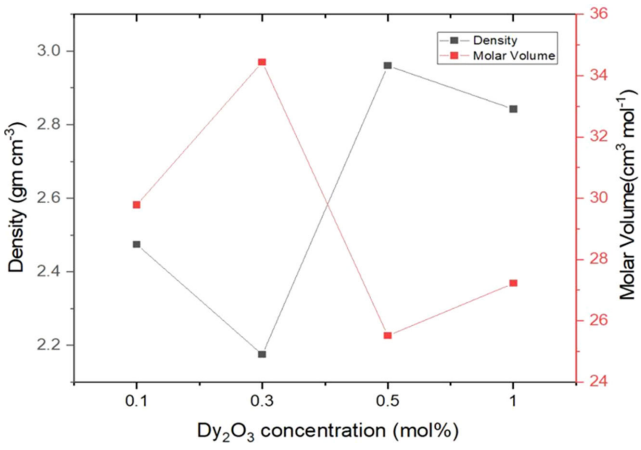

3.1.2. Average boron–boron distance

The average boron–boron separation (d_{B-B}) that identifies the effect of dopant concentration in the matrix is given.

$$(d_{B-B}) = \left(\frac{Vm}{2NA(1-Xp)}\right)^{1/3} \quad (1)$$

From Table 1, we can see that as the proportion of Dy_2O_3 has increased, the average spacing between boron and boron has also increased. Such an increase leads Dy atom to bond in between boron atoms. Hence, one can observe such increase in average boron to boron distance.

3.1.3. Interionic distance, polaron radius, and field strength

Dysprosium ion concentration (N_{Dy}), polaron radius (r_p), mean interionic distance (r_i), and field strength (F) are calculated by the relations.

$$N_{Dy} = (mol\%\ of\ Dy_2O_3)N_A\rho_g/M_w \quad (2)$$

$$Polaron\ radius, r_p = 0.5\left(\frac{\pi}{6N}\right)^{0.333} \quad (3)$$

$$\text{Interionic radii}, r_i = \left(\frac{1}{N}\right)^{0.333} \quad (4)$$

$$\text{Field strength}, F = \left(\frac{Z}{\text{rp2}}\right) \quad (5)$$

where N is the Dy^{3+} ion concentration.

From the measured values of refractive index (n) as shown in Table 1 and density, molar refractivity (R_M) and dielectric constant (ϵ) are calculated

$$R_{M=}\frac{(n2-1)}{(n2+2)}\left(\frac{M}{\rho}\right) \quad (6)$$

The drop in r_p and r_i that is seen as the Dy_2O_3 content rises is due to the rise in Dy^{3+} concentrations. As a result, the Dy-O distance decreases, increasing the Dy-O bond strength and, ultimately, the field strength surrounding the Dy^{3+} ion, as shown in Table 2.

3.1.4. Electronic oxide ion polarizability

From the refractive index (n), it is possible to calculate the oxide ion's electronic polarizability as follows:

$$\alpha_o{}^{2-}n = \left[\left(\frac{Vm}{2.52}\right)\left(\frac{(n2-1)}{(n2+2)}\right) - \sum\alpha_{cat}\right]/(N_o{}^{2-}) \quad (7)$$

where α cat denote the molar cation polarizability. These calculated values of $\alpha_o{}^{2-}$ and $N_o{}^{2-}$ are tabulated in Table 2. The refractive index method was used to calculate the electronic oxide polarizability using for the present glasses [8], and it was discovered that these values exhibit a nonlinear trend with increasing Dy_2O_3 content. This was anticipated due to the increase in NBO (non-bridging oxygen) in the current glass matrix [6]. As one can observe that the D2 glass shows more NBO's, the more oxide polarizability increases.

3.1.5. Metallization criteria (M)

The solid-state material's metallic or insulating behavior can be predicted using the metallization criterion, M, which is given by

$$M = 1 - (Rm/Vm) \quad (8)$$

The insulating behavior will be confirmed with $R_m < V_m$ and metallic behavior will be confirmed if $R_m > V_m$. The insulating behavior of the glasses is confirmed by evaluating the values of M, which are listed in Table 1.

3.1.6. Optical basicity

Glass's ability to transmit an ion's negative charge is evaluated using its optical basicity (the electron density carried by oxygen). The degree of basicity of oxide glass is proportional to the amount of oxygen that donates electrons. Bases are oxides having a low chemical hardness and a high electron density. Acids are compounds having a high chemical hardness and a low electron donation. The relationship between optical basicity and electronic oxide polarizability is given by

$$\Lambda = 1.67\left(1 - \frac{1}{\alpha_o{}^{2-}}\right) \quad (9)$$

It has been shown that the optical basicity displays a nonlinear trend with the increase of Dy_2O_3 content. These results indicate that electrical oxide polarizability and optical basicity are closely related, and that oxygen in contemporary glasses has a higher ability to transmit a negative charge to the surrounding cation.

3.1.7. Theoretical optical basicity

The following relation has been used to calculate the theoretical optical basicity (Λ_{theo}) of current glasses.

$$\Lambda_{theo} = xB_2O_3\Lambda B_2O_3 + XCaO\Lambda CaO + X\,Al_2O_3\Lambda Al_2O_3 + X\,BaO\Lambda BaO + XNa_2O\Lambda Na_2O + X\,Dy_2O_3\Lambda Dy_2O_3 \quad (10)$$

The optical basicity shows increases with increasing Dy_2O_3 content. The decrease in the theoretical optical basicity leads to a decrease in covalency of the cation oxygen bonds of the studied glasses.

3.2. IR studies

IR spectra can be used to study information about the rotation and vibration of different molecules in glass matrix. Since each group of molecules in the matrix has its own unique features of vibrational frequencies, each group's characteristic vibrations are related to frequency. These vibrations are independent of other groups of molecules present in the matrix. The images below show the CaAlBBaNaDy glasses' recorded Fourier transform infrared spectra at room temperature.

The spectrum shows seven typical bands coming from different elements in the current glasses doped with Dy^{3+} ions, and it depicts the functional groups of the glass matrix. The significant locational alterations in bands are shown in Figure 4. Peaks at 440, 583, 669, 834, 1255, 2920, and 3384 cm^{-1} were seen in the produced glass samples. The strength of these bands varies depending on the composition. The band in the range of 400–500 cm^{-1} is due to Ca^{2+} cation vibrations. Due to the existence of B-O bond stretching in the BO^{4-} structural unit from a di borate group, the second band was detected at 769–1200 cm^{-1}. The band seen between 1200 cm^{-1} and 1569 cm^{-1} is caused by the trigonal units of BO_3's NBOs stretching vibrations. The existence of symmetric hydrogen bond (OH) group vibrations in the referred glasses is what is responsible for the final strong wide band at 3384 cm^{-1} [9, 10].

Figure 4
FTIR of CaAlBBaNaDy glasses

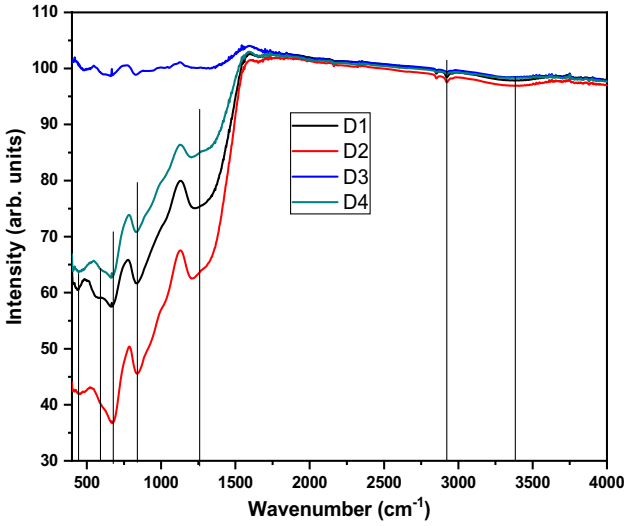

3.3. X-ray diffraction studies

The X-ray diffraction patterns of each glass sample doped with Dy^{3+} ions are shown in Figure 5. The diffracted intensity for the angular distribution of dispersed X-ray energy between 10° and 100° was measured for each sample. The XRD pattern clearly demonstrates the amorphous nature of all manufactured Dy^{3+} doped CaAlBBaNaDy glass samples by showing two significant broad humps [11].

Figure 5
X-ray diffraction pattern of CaAlBBaNaDy glasses

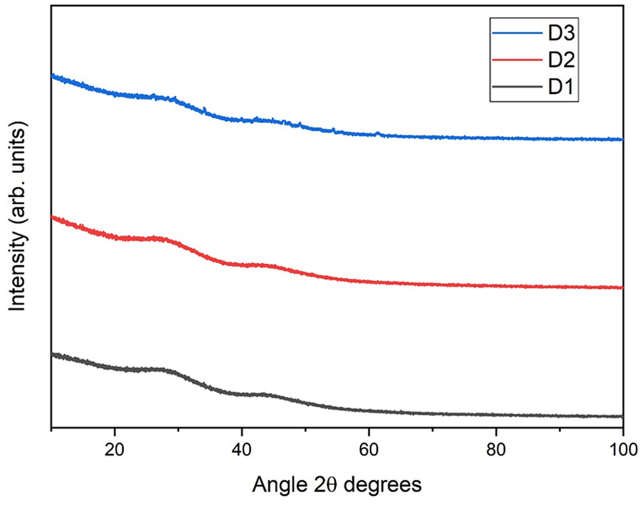

3.4. Optical absorption studies

In Figure 6, the absorption spectra reveals that the investigations of $23CaO + 10Al_2O_3 + (51–x)\ B_2O_3 + 6BaO + 10Na_2O + xDy_2O_3$ glass doped with different doses of Dy_2O_3 are determined. There are eleven absorption peaks in the spectrum, which are located at wavelengths of 346, 362, 384, 423, 450, 745, 796, 889, 1077, 1255, and 1667 nm and correspond to the electronic transitions of $^6P_{7/2}$, $^4P_{3/2}$, $^4F_{7/2}$, $^4G_{11/2}$, $^4I_{15/2}$, $^6F_{3/2}$, $^6F_{5/2}$, $^6F_{7/2}$, $^6F_{9/2}$, $^6H_{9/2}$, and $^6H_{11/2}$, respectively. In the produced CaAlBBaNaDy glass samples, the electronic transition at $^6H_{9/2}$ exhibits the maximum intensity in the 1255 nm NIR region [11, 12].

Figure 6
UV–Vis–NIR absorbance of CaAlBBaNaDy glasses

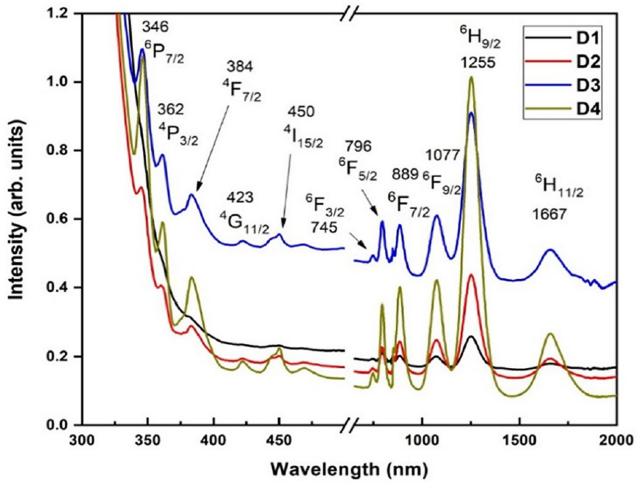

Figure 7
Direct optical band gap of CaAlBBaNaDy glasses

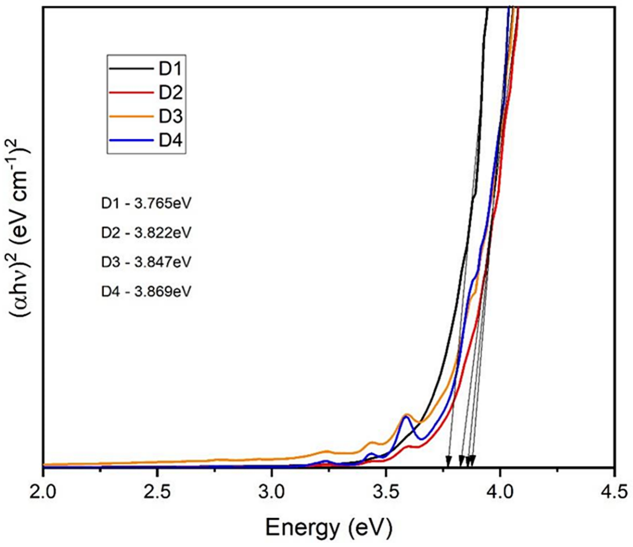

The optical band gap is evaluated and shows a direct energy band gap Eg_{direct} from 3.76 eV to 3.86 eV as shown in Figure 7, whereas the indirect energy band gap $Eg_{indirect}$ values have been evaluated and shown in Figure 8 using Tauc relation $\alpha h\nu = B(h\nu - E_g)^n$, where "B" represents constant, $h\nu$ is the energy, E_g represents band gap, and 'n' represents the transition process which adopts different values. When 'n' takes 2 for allowed transitions, 3 for indirect forbidden transitions, ½ for direct allowed transitions, and 3/2 for direct forbidden transitions. The values range from 3.39 eV to 3.45 eV as shown in Figure 8. The disorderness in the glass structure can be evaluated using the Urbach energy plot ln(α) vs hν graph (Figure 9) then taking the linear slope in the optical region and reciprocating gives the value of Urbach energy EU = 0.50 eV–0.58 eV and presented in Table 3. More disorderness

Figure 8
Indirect optical band gap of CaAlBBaNaDy glasses

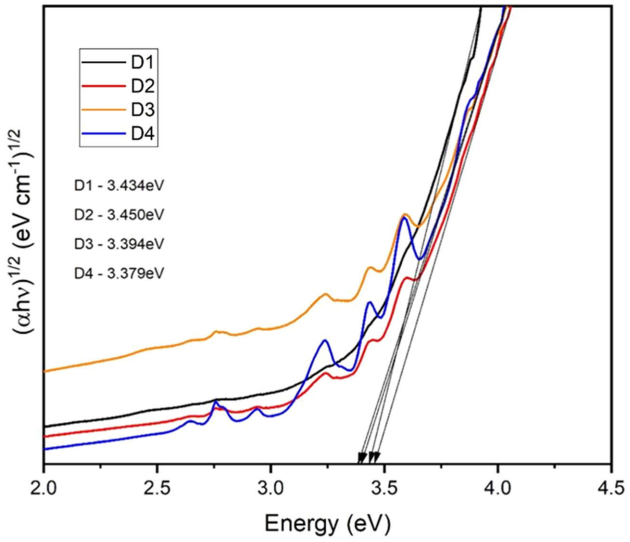

Figure 9
Urbach energy of CaAlBBaNaDy glasses

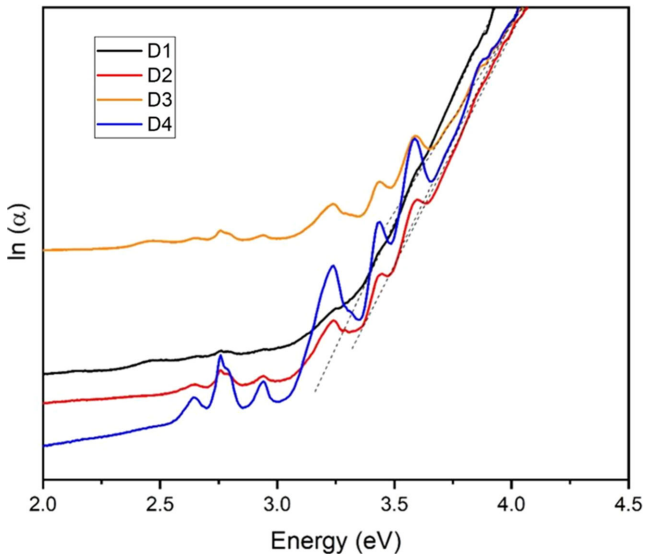

Figure 10
Photoluminescence spectra of excitation of CaAlBBaNaDy glasses

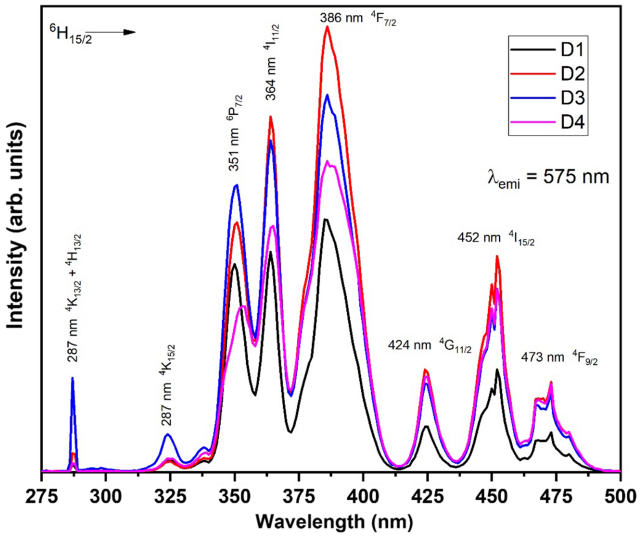

Figure 11
Photoluminescence spectra of emission of CaAlBBaNaDy glasses

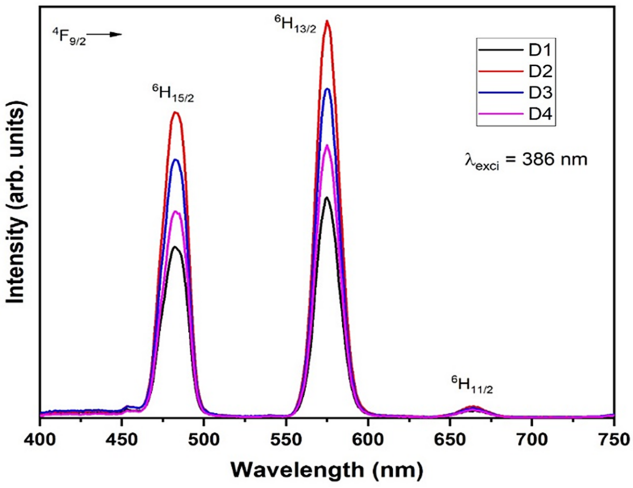

Table 3
Direct/indirect optical band gap and Urbach energy of the prepared glasses

Sl. no.	Glasses	Direct band gap (in eV)	Indirect band gap (in eV)	Urbach energy (E_U, eV)
01	(D1) CaAlBBaNaDy0.1	3.7060	3.085	0.53
02	(D2) CaAlBBaNaDy0.3	3.8717	3.589	0.58
03	(D3) CaAlBBaNaDy0.5	3.8664	3.500	0.54
04	(D4) CaAlBBaNaDy1.0	3.8672	3.450	0.50

was observed for D2 glass than compared to various Dy_2O_3 concentrations.

Figure 12
Partial energy level diagram of CaAlBBaNaDy glasses

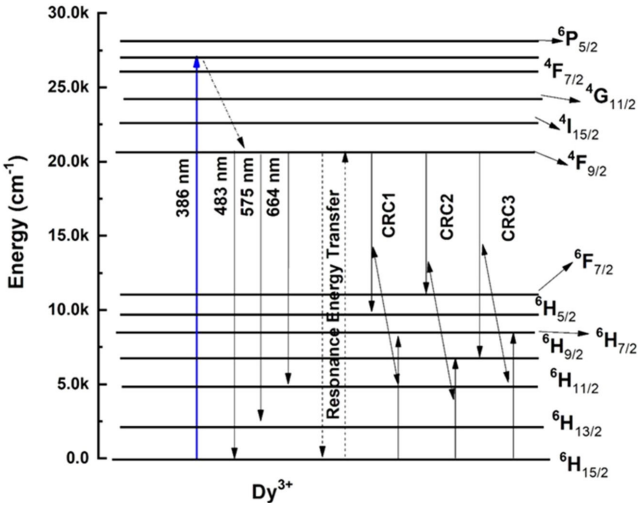

3.5. Luminescence studies

3.5.1. Photo-excitation spectra

The excitation spectra of the produced Dy^{3+} ions doped CaAlBBaNaDy glasses have been recorded spanning the wavelength range of 250–550 nm [13–16] by keeping watch of emission wavelengths at 575 nm and the excitation spectrum of CaAlBBaNaDy glass, as shown in Figure 10. Eight unique peaks were seen in the CaAlBBaNaDy glass excitation spectrum, which was recorded at 575 nm for emission. These peaks varied from the starting state ($^6H_{15/2}$) through many excited states ($^6P_{3/2}$), ($^6F_{5/2}$,$^4D_{5/2}$), ($^6P_{7/2}$, $^4M_{19/2}$+$^4P_{3/2}$,$^4D_{3/2}$), $^5P_{5/2}$, $^4F_{7/2}$+$^4I_{13/2}$, $^4G_{11/2}$, $^4I_{15/2}$, and $^4F_{9/2}$. The most potent peak in the excitation spectra of the glasses was determined to occur at 386 nm, leading researchers to conclude that effective excitation may be started by blue or near UV wavelengths, which are features of white light generations [13–16].

3.5.2. Photo-emission spectra

At an excitation wavelength of 386 nm, Figure 11 depicts the emission spectra of the studied glasses. It has three visible peaks that result from transitions from the $^4F_{9/2}$ to $^6H_{15/2}$ state,$^6H_{13/2}$ and $^6H_{11/2}$ states [13–16].

The emission spectrum under 386 nm excitation for $^4F_{9/2}$ to $^6H_{15/2}$ transitions, which are connected to electric and magnetic dipole transitions of Dy^{3+}, showed two strong bands in the blue and yellow region with maximums at 485 nm and 575 nm, as well as a minor red band at 645 nm. These transitions are also responsible for the 485 nm (blue) emission. The 575 nm (yellow) emission is caused by the $^4F_{9/2}$ to $^6H_{13/2}$ transition, which is linked to an electric dipole transition of Dy^{3+}. According to the PL emission spectrum, the yellow emission is greater than the blue emission in the Dy^{3+} doped CaAlBBaNaDy glasses. This demonstrates that a poor symmetrical spot in the current glass contains the REI Dy^{3+} [14, 17]. The concentration quenching effect was seen at a Dy_2O_3 level of 0.3 mol%. The Resonance Energy Transfer (RET) phenomenon luminescence intensity decreased, and as demonstrated in Figure 12, the activation of cross-relaxation pathways is also to blame for this (CRC).

Table 4
Judd–Ofelt parameters of the prepared CaAlBBaNaDy glasses

	(D1)		(D2)		(D3)		(D4)	
Wavelength	f_{exp}	f_{cal}	f_{exp}	f_{cal}	f_{exp}	f_{cal}	f_{exp}	f_{cal}
346	——	——	0.30	0.04	0.33	0.04	0.56	0.03
361	——	——	1.45	0.52	1.05	0.35	1.30	0.26
383	0.18	0.52	2.59	1.16	1.65	0.85	2.11	0.66
422	1.03	0.19	0.46	0.09	0.25	0.14	0.28	0.08
450	2.86	0.28	0.75	0.69	0.50	0.49	0.54	0.38
468	1.78	0.11	0.30	0.27	0.11	0.20	0.13	0.14
745	0.41	0.08	0.84	0.31	0.85	0.20	0.43	0.15
796	0.63	0.42	1.89	1.65	1.93	1.10	1.21	0.82
883	1.98	1.63	4.00	3.59	2.53	2.74	2.02	1.95
1077	3.36	3.45	3.80	3.89	3.83	3.80	2.50	2.53
1252	0.90	9.00	8.57	8.52	8.14	8.12	6.68	6.65
1657	0.63	0.95	1.59	1.94	1.27	1.45	0.91	1.13
N	10		12		12		12	
RI	1.58		1.58		1.57		1.58	
δ_{rms}	0.988		0.556		0.447		0.548	
Ω_2 ($\times10^{-20}$)	8.382		7.183		6.793		6.219	
Ω_4 ($\times10^{-20}$)	5.461		2.611		4.108		2.453	
Ω_6 ($\times10^{-20}$)	1.011		3.965		2.666		1.969	
JO Trend	$\Omega_2 > \Omega_4 > \Omega_6$		$\Omega_2 > \Omega_6 > \Omega_4$		$\Omega_2 > \Omega_4 > \Omega_6$		$\Omega_2 > \Omega_4 > \Omega_6$	

3.5.3. Judd–Ofelt analysis

The Judd–Ofelt intensity parameters (Ω_λ, where $\lambda = 2,4,6$) have been evaluated using the absorption spectra of synthesized Dy^{3+} doped CaAlBBaNaDy glasses. The results are shown in Table 4, which demonstrates that the J-O parameters consistently follow the trend of $\Omega_2 > \Omega_4 > \Omega_6$ for all the current glass samples. The J-O intensity characteristic Ω2 is more sensitive to the local structure around the rare-earth ions (Dy^{3+}) and is most reliant on the properties of the glasses, such as viscosity and rigidity. It has been shown that the J-O intensity characteristics of the tested glasses are identical to those of known Dy^{3+} doped glasses [13, 14, 16].

3.5.4. Radiative transition properties

Using J-O parameters, emission spectra, and refractive index, radiative characteristics including stimulated emission

Table 5
Comparison of J-O parameters ($\times 10^{-20}$ cm^2) with other Dy doped glasses

Sl.no.	Glass	Ω_2 ($\times 10^{-20}$)	Ω_4 ($\times 10^{-20}$)	Ω_6 ($\times 10^{-20}$)	J-O trend	References
1	CaAlBBaNaDy0.1	8.382	5.461	1.011	$\Omega_2 > \Omega_4 > \Omega_6$	Present glass
2	CaAlBBaNaDy 0.3	7.183	2.611	3.965	$\Omega_2 > \Omega_6 > \Omega_4$	Present glass
3	CaAlBBaNaDy 0.5	6.793	4.108	2.666	$\Omega_2 > \Omega_4 > \Omega_6$	Present glass
4	CaAlBBaNaDy 1.0	6.219	2.453	1.969	$\Omega_2 > \Omega_4 > \Omega_6$	Present glass
5	Borate (0.8 mol%)	16.09	3.67	2.61	$\Omega_2 > \Omega_4 > \Omega_6$	Venkata Rao et al. [15]
6	$(NaPO_3)_6$-TeO_2-AlF_3-LiF	7.06	2.20	0.97	$\Omega_2 > \Omega_4 > \Omega_6$	Carnall et al. [13]
7	0.05LBTPD	8.64	4.43	3.46	$\Omega_2 > \Omega_4 > \Omega_6$	Selvi et al. [16]
8	LMgBDy05	9.60	5.83	5.82	$\Omega_2 > \Omega_4 > \Omega_6$	Narwal et al. [14]
9	L4BD	9.85	4.35	2.47	$\Omega_2 > \Omega_4 > \Omega_6$	Babu and Jayasankar [17]
10	0.5Dy	10.69	4.81	5.17	$\Omega_2 > \Omega_6 > \Omega_4$	Praveena et al. [19]
11	0.1DyBBCZFB	6.747	2.389	2.202	$\Omega_2 > \Omega_4 > \Omega_6$	Mariselvam and Liu [20]
12	Dy:LiLTB	8.75	2.62	2.07	$\Omega_2 > \Omega_4 > \Omega_6$	Saleem et al. [21]
13	ZP1D	7.30	1.14	0.86	$\Omega_2 > \Omega_4 > \Omega_6$	Lira et al. [22]
14	BPAPbLiDy0.1	5.0624	2.1889	2.5195	$\Omega_2 > \Omega_6 > \Omega_4$	Joseph et al. [23]
15	Dy_0.5	19.85	6.66	8.64	$\Omega_2 > \Omega_6 > \Omega_4$	Rajagukguk et al. [24]
16	BGGD	3.11	0.84	1.87	$\Omega_2 > \Omega_6 > \Omega_4$	Gökçe and Koçyiğit [25]
17	Dy01	6.1242	1.2689	1.2299	$\Omega_2 > \Omega_4 > \Omega_6$	Tayal and Rao [26]
18	MgB2O3Dy0.2	17.62	12.36	10.84	$\Omega_2 > \Omega_4 > \Omega_6$	Ichoja et al. [9]

hypersensitive transition. The hypersensitive transitions with greater relative oscillator strength value cause the higher Ω_2 value. A much larger value of the Ω_4 parameter suggests increased stiffness in the glass network of the generated glasses as compared to Linganna et al. [12], Venkata Rao et al. [15] and Rajaramakrishna et al. [18] and presented in Table 5. The Ω_4 and Ω_6 parameters are related to the bulk cross-section (σ), radiative transition probability (A_R), estimated and experimental, and calculated branching ratio (β) were identified [27]. The findings of D series glasses for the transitions $^4F_{9/2} \rightarrow {}^6H_J$ (J = 15/2, 13/2, and 11/2) are shown in Table 6. When using low threshold high gain lasers, the stimulated emission cross-section (σ) is a crucial parameter.

Table 6
Radiative properties of prepared glass samples

Radiative properties	D1	D2	D3	D4
		482 nm		
$\Delta\lambda_{eff}$ (nm)	16.95	18.66	13.83	17.19
A_R (s^{-1})	139.81	323.02	240.38	174.29
σ (cm^2) × 10^{-20}	0.337	0.859	0.4738	0.4268
β_{exp}	0.46	0.45	0.37	0.45
β_{Cal}	0.11	0.22	0.19	0.17
		575 nm		
$\Delta\lambda_{eff}$ (nm)	15.08	16.62	17.88	14.83
A_R (s^{-1})	769.9	29.14	767.54	849.31
σ (cm^2) × 10^{-20}	3.467	4.207	3.960	3.635
β_{exp}	0.52	0.53	0.61	0.52
β_{Cal}	0.65	0.60	0.61	0.62
		664 nm		
$\Delta\lambda_{eff}$ (nm)	16.73	13.86	13.86	14.82
A_R (s^{-1})	97.43	91.39	114.72	276.41
σ (cm^2) × 10^{-20}	0.836	0.6501	0.816	2.10
β_{exp}	0.02	0.01	0.01	0.01
β_{Cal}	0.08	0.06	0.07	0.07

Table 7
Radiative properties of present glasses and compared with other Dy^{3+} doped glasses

Glass	$\Delta\lambda_{eff}$ (nm)	A_R (s^{-1})	σ (cm^2) × 10^{-20}	β_{exp}	β_{Cal}	References
			λ = 482nm			
CaAlBBaNaDy0.1	16.95	139.81	0.337	0.46	0.11	Present work
CaAlBBaNaDy0.3	18.66	223.02	0.859	0.45	0.22	Present work
CaAlBBaNaDy0.5	13.83	240.38	0.4738	0.37	0.19	Present work
CaAlBBaNaDy1.0	17.19	174.29	0.4268	0.45	0.17	Present work
BLCFDy3	16.536	165.55	0.0448	0.0692	0.1058	Nishiura and Tanabe [4]
0.05LBTPD	9.38	350.8	8.71	0.610	0.635	Selvi et al. [16]
LMgBDy05	18.67	419.14	6.49	0.40	0.24	Narwal et al. [14]
BGGD1.00	19.77	253.53	3.10	0.320	0.213	Gökçe and Koçyiğit [25]
C2	16.29	440.31	1.1176	0.49	0.20	Rajaramakrishna et al. [28]
D	16.39	489.11	0.5837	0.48	0.21	Rajaramakrishna et al. [28]
CSPB:1.0Dy	20.00	161.68	0.0104		0.22	Albaqawi et al. [29]
1.0DSrMB		1725.7	1.78		0.24	Ichoja et al. [27]
BTKA0.05D	6 ± 1	70.77	2.84	0.126 ± 0.0007	0.109	Annapoorani et al. [30]
			λ = 575 nm			
CaAlBBaNaDy0.1	15.08	769.9	3.467	0.52	0.65	Present work
CaAlBBaNaDy0.3	16.62	29.14	4.207	0.53	0.60	Present work
CaAlBBaNaDy0.5	17.88	767.54	3.960	0.61	0.61	Present work
CaAlBBaNaDy1.0	14.83	849.31	3.635	0.52	0.62	Present work
BLCFDy3	15.006	492.31	0.2973	0.5841	0.8941	Nishiura and Tanabe [4]
0.05LBTPD	6.68	1193.1	84.04	0.357	0.213	Selvi et al. [16]
LMgBDy05	17.76	1031.26	33.98	0.56	0.60	Narwal et al. [14]
BGGD1.00	19.51	835.56	20.93	0.723	0.703	Gökçe and Koçyiğit [25]
C2	16.44	1425.3	6.869	0.50	0.70	Rajaramakrishna et al. [28]
D	18.91	1412.81	4.8265	0.50	0.69	Rajaramakrishna et al. [28]
CSPB:1.0Dy	13.00	498.94	0.1015		0.71	Albaqawi et al. [29]
1.0DSrMB		5286.5	35.56		0.73	Ichoja et al. [27]
BTKA0.05D	5 ± 1	395.08	38.56	0.850 ± 0.0017	0.609	Annapoorani et al. [30]
			λ = 664 nm			
CaAlBBaNaDy0.1	16.73	97.43	0.836	0.02	0.08	Present work
CaAlBBaNaDy0.3	13.86	91.39	0.650	0.01	0.06	Present work
CaAlBBaNaDy0.5	13.86	14.72	0.816	0.01	0.07	Present work
CaAlBBaNaDy1.0	14.82	276.41	2.10	0.01	0.07	Present work
BLCFDy3	14.799	58.3	0.0634	0.1964	0.3006	Nishiura and Tanabe [4]
0.05LBTPD	13.23	208.9	13.27	0.033	0.063	Selvi et al. [16]
LMgBDy05	15.37	96.45	6.53	0.02	0.06	Narwal et al. [14]
BGGD1.00	21.00	80.03	3.27	0.069	0.067	Gökçe and Koçyiğit [25]
C2	9.35	149.82	0.721	0.01	0.06	Rajaramakrishna et al. [28]
D	15.71	144.13	0.789	0.01	0.06	Rajaramakrishna et al. [28]
CSPB:1.0Dy	14.00	48.20	0.0151		0.06	Albaqawi et al. [29]
BTKA0.05D	8±1	57.99	6.17	0.019 ± 0.0007	0.089	Annapoorani et al. [30]

The maximum stimulated emission cross-section value for the highest emission peak, 575 nm, is found in the D2 glass sample, per Table 6. Table 7 compares it to other published publications as well as the inside of the glass sample.

3.5.5. Asymmetry (Y/B) ratio

The Y/B emission peak ratio for the present glasses, which was found to be in the range of 1.257 to 1.316, was used to compute the asymmetry value and was then compared to previous published findings. The produced glass samples fall within the same range as the other evaluated and listed glasses are presented in Table 8. Variations in the Y/B value might be used to customize and tailor the purity of white emission.

Table 8
Asymmetry ratio of Dy^{3+} doped glasses

Glass	Y/B ratio	References
CaAlBBaNaDy0.1	1.316	Present work
CaAlBBaNaDy0.3	1.299	Present work
CaAlBBaNaDy0.5	1.267	Present work
CaAlBBaNaDy1.0	1.315	Present work
0.8Dy	1.10	Lv et al. [31]
NPABSDy5	1.063	Vijaya Babu and Cole [32]
LZBSDy0.1	2.35	Jaidass et al. [33]
BiBTDy0.1	1.642	Lakshmi et al. [34]
DY0.1	1.66	Monisha et al. [35]

Table 9
CIE chromatically coordinates, and CCT(K) for CaAlBBaNaDy glasses

Glass	*X*	*Y*	CCT (K)	D_{UV}	References
CaAlBBaNaDy0.1	0.3493	0.3828	4957	0.0133	Present work
CaAlBBaNaDy0.3	0.3518	0.3882	4894	0.0148	Present work
CaAlBBaNaDy0.5	0.3490	0.3846	4970	0.0142	Present work
CaAlBBaNaDy1.0	0.3546	0.3922	4824	0.0156	Present work
KD	0.386	0.401	4022	0.009	Divina et al. [36]
NaD	0.397	0.427	3928	0.017	Divina et al. [36]
CaD	0.391	0.421	4022	0.016	Divina et al. [36]
SrD	0.351	0.415	4978	0.027	Divina et al. [36]
BaD	0.333	0.383	5485	0.056	Divina et al. [36]
L15(Oxyfluoride)	0.347	0.380	5016	0.013	Lakshminarayana et al. [37]

Figure 13
CIE chromaticity diagram of D series glasses

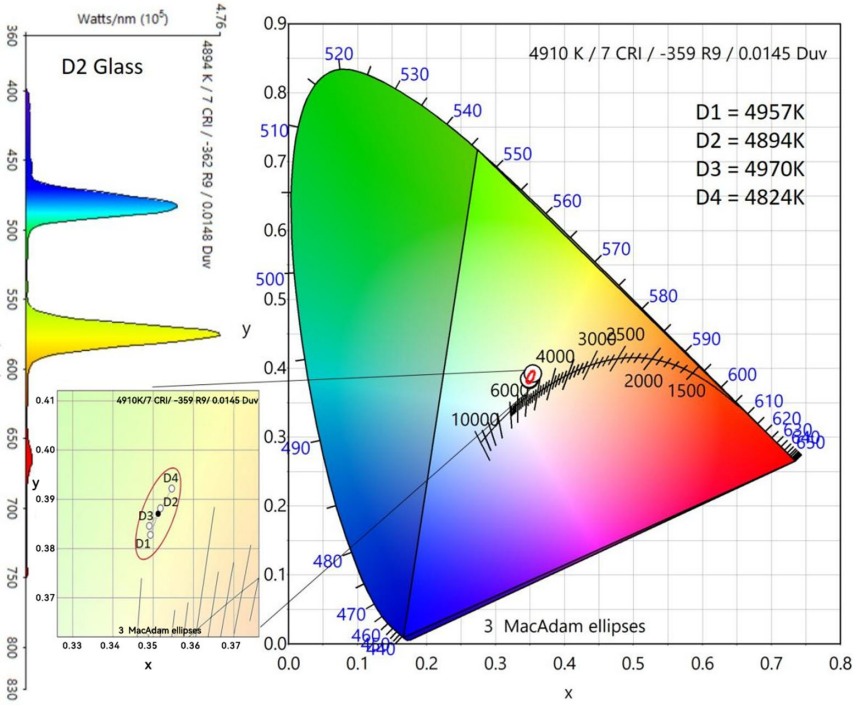

3.6. CIE color chromaticity diagram

The glass samples under examination were studied using a color coordinate system using the CIE 1931 chromaticity diagram. The doped rare-earth ions in the current study have a specific effect on the luminescence color of the examined materials triggered at 386 nm. According to the analysis, the dimensions of Dy^{3+} ions are around $x = 0.34$–0.35; $y = 0.38$–0.39, as shown in Table 9 and Figure 13. These color coordinates (x, y) from the CIE diagram are used to determine the co-related color temperature (CCT) value [34]. With the D1, D2, D3, and D4 glasses, the CCT values were 4957 K, 4894 K, 4970 K, and 4824 K, respectively.

These findings imply that the investigated glasses generate white light at an excitation wavelength of 386 nm. The produced glass samples exhibit exceptional temperature resistance, which is a prerequisite for applications involving solid-state lighting devices.

Delta u,v (D_{uv}) is a significant number that displays the separation of a light color point from the black body radiation curve and is usually associated with CCT values in revealing the black body curve's closeness to a specific light source [36, 37]. D_{uv}, like CCT, is an important metric that provides combined scale and orientation information about a color-sensitive lighting application, such as film and photography. This number is in the ±0.003 range. D_{uv} values were determined using expressions found in Ohno [38]. As with the current glasses, D_{uv} values are positive, indicating that the color-emitted photons of the glasses deviate out from black body profile but are more centered and are more situated in the yellow region of CIE 1931 diagram.

4. Conclusions

Density and molar volume of the glasses exhibit an inverse trend, showing that as the concentration of Dy_2O_3 rises, more non-bridging oxygen is present in the glasses. The BO_4 structural unit from a diborate group and stretching vibrations of NBOs from BO_3 trigonal units are both visible in FTIR. Urbach energy

showed that the D2 glass sample was more disorderly. Judd–Ofelt theory was used to highlight the importance of Ω_λ ($\lambda = 2,4,6$), and it was discovered that they follow the $\Omega_2 > \Omega_4 > \Omega_6$ trend, whereas D2 follows the $\Omega_2 > \Omega_6 > \Omega_4$ trend. When compared, the stimulated emission cross-section values at 575 nm were greater. Pure white emission might be tuned using variations in the peak-to-peak ratio of the asymmetric (Yellow/Blue) emission. The CCT values seem to be similar and are in the 4824–4970 K range. The color coordinates (x, y) and D_{uv} also display values that are similar, indicating that these produced glasses may be employed for solid-state applications involving white light-emitting (*w*-LED) devices.

Ethical Statement

This study does not contain any studies with human or animal subjects performed by any of the authors.

Conflicts of Interest

The authors declare that they have no conflicts of interest to this work.

Data Availability Statement

Data are available from the corresponding author upon reasonable request.

Author Contribution Statement

Basavaraj Gurav: Software, Formal analysis, Investigation, Resources, Data curation, Writing – original draft, Writing – review & editing, Visualization. **G. B. Devidas:** Validation, Project administration. **Ashok Dinkar:** Software, Formal analysis, Investigation, Resources, Data curation, Writing – original draft, Writing – review & editing. **Darya Pavlovna Surzhikova:** Software, Investigation. **R. Rajaramakrishna:** Conceptualization, Methodology, Validation, Writing – review & editing, Supervision, Project administration.

References

[1] Carreira, J. F. C., Sava, B. A., Boroica, L., Elisa, M., Stefan, R., Monteiro, R. C. C., . . . , & Rino, L. (2019). Structural and luminescence characterization of a Dy/Tb co-doped borophosphate glass. *Journal of Non-Crystalline Solids*, *526*, 119719. https://doi.org/10.1016/j.jnoncrysol.2019.119719

[2] Zhang, Y., Hao, Z., Yang, A., Wu, Y., Zhu, W., Xu, H., & Peng, D. (2024). Influence of CaF_2 on the spectroscopic studies of Dy–Eu co-doped fluoroborate glass for lighting applications. *Ceramics International*, *50*(2), 3074–3083. https://doi.org/10.1016/j.ceramint.2023.11.055

[3] Fernández-Rodríguez, L., Allix, M., Gorni, G., Canizarès, A., Ory, S., Mather, G. C., . . . , & Pascual, M. J. (2022). Persistent luminescence of Eu/Dy-doped $Sr_2MgSi_2O_7$ glass-ceramics processed by aerodynamic levitation. *Journal of the European Ceramic Society*, *42*(16), 7596–7608. https://doi.org/10.1016/j.jeurceramsoc.2022.08.062

[4] Nishiura, S., & Tanabe, S. (2009). Preparation and luminescence properties of glass ceramics precipitated with $M_2MgSi_2O_7$: Eu^{2+} (M = Sr, Ca) phosphor for white light source. *IEEE Journal of Selected Topics in Quantum Electronics*, *15*(4), 1177–1180. http://dx.doi.org/10.1109/JSTQE.2009.2014175

[5] Yin, T., Lepry, W. C., Hudon, P., Ouzilleau, P., Waters, K. E., & Nazhat, S. N. (2023). Mechanism of dissolution reactivity and reactions of various calcium borate glasses and glass-ceramics. *Journal of Non-Crystalline Solids*, *614*, 122406. https://doi.org/10.1016/j.jnoncrysol.2023.122406

[6] Zeed, M. A., Saeed, A., El Shazly, R. M., El-Mallah, H. M., & Elesh, E. (2023). Double effect of glass former B_2O_3 and intermediate Pb_3O_4 augmentation on the structural, thermal, and optical properties of borate network. *Optik*, *272*, 170368. https://doi.org/10.1016/j.ijleo.2022.170368

[7] Kaewjaeng, S., Kothan, S., Chaiphaksa, W., Chanthima, N., Rajaramakrishna, R., Kim, H. J., & Kaewkhao, J. (2019). High transparency La_2O_3-CaO-B_2O_3-SiO_2 glass for diagnosis x-rays shielding material application. *Radiation Physics and Chemistry*, *160*, 41–47. https://doi.org/10.1016/j.radphyschem.2019.03.018

[8] Dimitrov, V., & Komatsu, T. (2010). An interpretation of optical properties of oxides and oxide glasses in terms of the electronic ion polarizability and average single bond strength. *Journal of the University of Chemical Technology and Metallurgy*, *45*(3), 219–250.

[9] Ichoja, A., Hashim, S., Ghoshal, S. K., Hashim, I. H., & Omar, R. S. (2018). Physical, structural and optical studies on magnesium borate glasses doped with dysprosium ion. *Journal of Rare Earths*, *36*(12), 1264–1271. https://doi.org/10.1016/j.jre.2018.05.013

[10] Sadeq, M. S., AlHammad, M. S., & Al-Wafi, R. (2024). Effect of samarium oxide on the structural and ligand field parameters of iron cations inside sodium borate glass. *Ceramics International*, *50*(1), 115–125. https://doi.org/10.1016/j.ceramint.2023.10.028

[11] Koçyiğit, D., Gökçe, M., & Gökçe, A. G. (2024). The impact of heat treatment on the luminescence properties of Dy/Ag co-doped sodium alumina borate glasses. *Materials Chemistry and Physics*, *315*, 128916. https://doi.org/10.1016/j.matchemphys.2024.128916

[12] Linganna, K., Srinivasa Rao, C., & Jayasankar, C. K. (2013). Optical properties and generation of white light in Dy^{3+}-doped lead phosphate glasses. *Journal of Quantitative Spectroscopy and Radiative Transfer*, *118*, 40–48. https://doi.org/10.1016/j.jqsrt.2012.12.002

[13] Carnall, W. T., Fields, P. R., & Rajnak, K. (1968). Electronic energy levels in the trivalent lanthanide aquo ions. I. Pr^{3+}, Nd^{3+}, Pm^{3+}, Sm^{3+}, Dy^{3+}, Ho^{3+}, Er^{3+}, and Tm^{3+}. *The Journal of Chemical Physics, 49*(10), 4424–4442. https://doi.org/10.1063/1.1669893

[14] Narwal, P., Dahiya, M. S., Yadav, A., Hooda, A., Agarwal, A., & Khasa, S. (2017). Dy^{3+} doped LiCl–CaO–Bi_2O_3–B_2O_3 glasses for WLED applications. *Ceramics International*, *43*(14), 11132–11141. https://doi.org/10.1016/j.ceramint.2017.05.160

[15] Venkata Rao, K., Babu, S., Venkataiah, G., & Ratnakaram, Y. C. (2015). Optical spectroscopy of Dy^{3+} doped borate glasses for luminescence applications. *Journal of Molecular Structure*, *1094*, 274–280. https://doi.org/10.1016/j.molstruc.2015.04.015

[16] Selvi, S., Venkataiah, G., Arunkumar, S., Muralidharan, G., & Marimuthu, K. (2014). Structural and luminescence studies on Dy^{3+} doped lead boro–telluro-phosphate glasses. *Physica B: Condensed Matter*, *454*, 72–81. https://doi.org/10.1016/j.physb.2014.07.018

[17] Babu, P., & Jayasankar, C. K. (2000). Spectroscopic properties of Dy^{3+} ions in lithium borate and lithium fluoroborate glasses. *Optical Materials*, *15*(1), 65–79. https://doi.org/10.1016/S0925-3467(00)00015-X

[18] Rajaramakrishna, R., Knorr, B., Dierolf, V., Anavekar, R. V., & Jain, H. (2014). Spectroscopic properties of Sm^{3+}-doped lanthanum borogermanate glass. *Journal of Luminescence*, *156*, 192–198. https://doi.org/10.1016/j.jlumin.2014.07.021

[19] Praveena, R., Vijaya, R., & Jayasankar, C. K. (2008). Photoluminescence and energy transfer studies of Dy^{3+}-doped fluorophosphate glasses. *Spectrochimica Acta Part A: Molecular and Biomolecular Spectroscopy*, *70*(3), 577–586. https://doi.org/10.1016/j.saa.2007.08.001

[20] Mariselvam, K., & Liu, J. (2021). Spectroscopic and radiative properties of Dy^{3+}: BBCZFB glass suitable for solid-state yellow laser and W-LEDs applications. *Optics & Laser Technology*, *140*, 106944. https://doi.org/10.1016/j.optlastec.2021.106944

[21] Saleem, S. A., Jamalaiah, B. C., Jayasimhadri, M., Srinivasa Rao, A., Jang, K., & Rama Moorthy, L. (2011). Luminescent studies of Dy^{3+} ion in alkali lead tellurofluoroborate glasses. *Journal of Quantitative Spectroscopy and Radiative Transfer*, *112*(1), 78–84. https://doi.org/10.1016/j.jqsrt.2010.08.017

[22] Lira, A., Speghini, A., Camarillo, E., Bettinelli, M., & Caldiño, U. (2014). Spectroscopic evaluation of $Zn(PO_3)_2$: Dy^{3+} glass as an active medium for solid state yellow laser. *Optical Materials*, *38*, 188–192. https://doi.org/10.1016/j.optmat.2014.10.024

[23] Joseph, P. A. J., Maheshvaran, K., & Arul Rayappan, I. (2021). Structural and optical studies on Dy^{3+} ions doped alkali lead borophosphate glasses for white light applications. *Journal of Non-Crystalline Solids*, *557*, 120652. https://doi.org/10.1016/j.jnoncrysol.2021.120652

[24] Rajagukguk, J., Yuliantini, L., Fitrilawati, Djamal, M., & Kaewkhao, J. (2020). Investigation of Dy^{3+} ion doped borate glasses and their potential for WLED and laser application. *Journal of Engineering and Technological Sciences*, *52*(6), 891–906.

[25] Gökçe, M., & Koçyiğit, D. (2019). Spectroscopic investigations of Dy^{3+} doped borogermanate glasses for laser and wLED applications. *Optical Materials*, *89*, 568–575. https://doi.org/10.1016/j.optmat.2019.02.004

[26] Tayal, Y., & Rao, A. S. (2021). Spectroscopic analysis of Dy^{3+} ions activated borosilicate glasses for photonic device applications. *Optical Materials*, *117*, 111112. https://doi.org/10.1016/j.optmat.2021.111112

[27] Ichoja, A., Hashim, S., & Ghoshal, S. K. (2020). Judd–Ofelt calculations for spectroscopic characteristics of Dy^{3+}-activated strontium magnesium borate glass. *Optik*, *218*, 165001. https://doi.org/10.1016/j.ijleo.2020.165001

[28] Rajaramakrishna, R., Ruangtaweep, Y., Sattayaporn, S., Kidkhunthod, P., Kothan, S., & Kaewkhao, J. (2020). Structural analysis and luminescence studies of Ce^{3+}: Dy^{3+} co-doped calcium zinc gadolinium borate glasses using EXAFS. *Radiation Physics and Chemistry*, *171*, 108695. https://doi.org/10.1016/j.radphyschem.2020.108695

[29] Albaqawi, H. S., AL-Shomar, S. M., Danmallam, I. M., & Bulus, I. (2023). Judd-Ofelt analysis and luminescence properties of newly fabricated Dy^{3+} infused calcium sulfo-phospho-borate glasses for photonics applications. *Journal of Alloys and Compounds*, *965*, 171101. https://doi.org/10.1016/j.jallcom.2023.171101

[30] Annapoorani, K., Karthikeyan, P., Basavapoornima, C., & Marimuthu, K. (2017). Investigations on the optical properties of Dy^{3+} ions doped potassium aluminiumtelluroborate glasses for white light applications. *Journal of Non-Crystalline Solids*, *476*, 128–136. https://doi.org/10.1016/j.jnoncrysol.2017.09.038

[31] Lv, H., Wang, S., Su, C., Zhang, H., Guo, Z., Wang, L., . . . , & Wei, Y. (2020). Preparation and luminescence properties of Dy^{3+}-doped transparent glass–ceramics containing $NaGd(WO_4)_2$. *Journal of Materials Science: Materials in Electronics, 31*(9), 6636–6644. https://doi.org/10.1007/s10854-020-03219-8

[32] Vijaya Babu, K., & Cole, S. (2018). Luminescence properties of Dy^{3+}-doped alkali lead alumino borosilicate glasses. *Ceramics International*, *44*(8), 9080–9090. https://doi.org/10.1016/j.ceramint.2018.02.115

[33] Jaidass, N., Moorthi, C. K., Babu, A. M., & Babu, M. R. (2018). Luminescence properties of Dy^{3+} doped lithium zinc borosilicate glasses for photonic applications. *Heliyon*, *4*(3), e00555. https://doi.org/10.1016/j.heliyon.2018.e00555

[34] Lakshmi, Y. A., Swapna, K., Rama Krishna Reddy, K. S., Mahamuda, S., Venkateswarulu, M., & Rao, A. S. (2020). Concentration dependent photoluminescence studies of Dy^{3+} doped Bismuth Boro-Tellurite glasses for lasers and wLEDs. *Optical Materials*, *109*, 110328. https://doi.org/10.1016/j.optmat.2020.110328

[35] Monisha, M., Mazumder, N., Lakshminarayana, G., Mandal, S., & Kamath, S. D. (2021). Energy transfer and luminescence study of Dy^{3+} doped zinc-aluminoborosilicate glasses for white light emission. *Ceramics International*, *47*(1), 598–610. https://doi.org/10.1016/j.ceramint.2020.08.167

[36] Divina, R., Teresa, P. E., & Marimuthu, K. (2021). Dy^{3+} ion as optical probe to study the luminescence behavior of Alkali lead bismuth borate glasses for w-LED application. *Journal of Alloys and Compounds*, *883*, 160845. https://doi.org/10.1016/j.jallcom.2021.160845

[37] Lakshminarayana, G., Vighnesh, K. R., Prabhu, N. S., Lee, D.-E., Yoon, J., Park, T., & Kamath, S. D. (2020). Dy^{3+}: B_2O_3–Al_2O_3–ZnF_2–NaF/LiF oxyfluoride glasses for cool white or day white light-emitting applications. *Optical Materials*, *108*, 110186. https://doi.org/10.1016/j.optmat.2020.110186

[38] Ohno, Y. (2014). Practical use and calculation of CCT and Duv. *LEUKOS*, *10*(1), 47–55. https://doi.org/10.1080/15502724.2014.839020

How to Cite: Gurav, B., Devidas, G. B., Dinkar, A., Surzhikova, D. P., & Rajaramakrishna, R. (2025). Instigating the Asymmetry of Dy^{3+} Ions Doped in Borate Glasses for Photonic Device *w*-LED Applications. *Journal of Optics and Photonics Research*. https://doi.org/10.47852/bonviewJOPR42022256